Supplementary Information

Supramolecular Assembly of a Poly(ionic liquid) ABC Triblock Copolymer with Monovalent Halogen Bond Donors

Abena A. Adjei,[a] Mark Potter,[b] Chandan Giri,[a] Tiago C. Gomes,[b] Simon Rondeau-Gagné,[b] Ngong Kodiah Beyeh.*[a]*

[a] Department of Chemistry, Oakland University, 146 Library Drive, Rochester, MI 48309-4479, USA

[b] Department of Chemistry & Biochemistry, University of Windsor, 401 Sunset Ave, Windsor, ON N9B 3P4, Canada

Table of Contents

1. Materials

All reagents were purchased from Sigma-Aldrich and were used as received. Organic solvents were purchased from Sigma-Aldrich and Pharmco. Monomers for polymerizations were first filtered over neutral alumina to remove stabilizers before use.

2. Synthesis

Synthesis of 2-Hydroxyethyl phenylmethyl carbonotrithioate Chain Transfer Agent (CTA).

The CTA was synthesized according to previously reported procedures.[1] In summary, 1 equivalent of 2-mercaptoethanol (1.00 g, 12.82 mmol) was combined with 1 equivalent of tripotassium phosphate (2.71 g, 12.82 mmol) in acetone (20.00 mL) at room temperature. After 10 minutes, 3 equivalents of carbon disulfide (2.92 g, 38.46 mmol) were added and stirred for an additional 10 minutes to form a bright yellow mixture. 1 equivalent of benzyl bromide (2.91 g, 12.82 mmol) was then added and stirred for 5 minutes. Potassium bromide side product was filtered and washed with acetone. The solvent was removed from the filtrate under reduced pressure, and the resulting yellow residue was purified via column chromatography on silica using a petroleum ether/ethyl acetate gradient. This produced a bright yellow oil (yield = 91%) that crystallized upon refrigeration. δH (400 MHz, CDCl3) = 7.24-7.22 (5H, d, Ph), 4.25 (2H, s, CH_2), 3.78 (2H, s, CH_2), 3.52-3.49 (2H, t, CH_2).

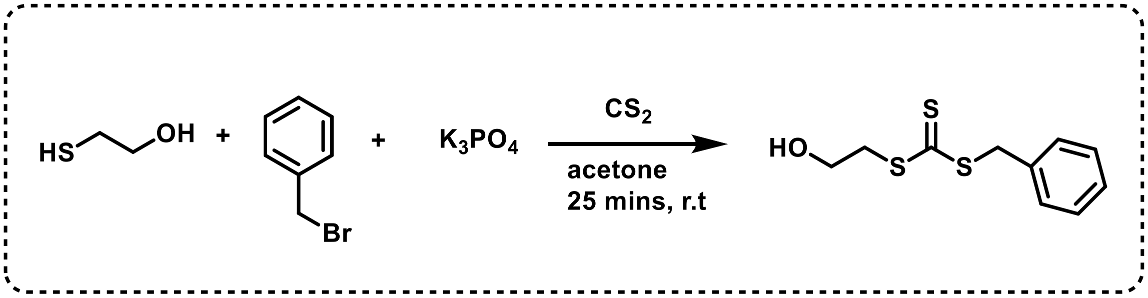

Scheme S1. Synthesis of 2-Hydroxyethyl phenylmethyl carbonotrithioate Chain Transfer Agent (CTA)

RAFT Polymerization Reactions

All monomers, precursors (CTA or polymer macro-CTA), and initiator; 2,2′-Azobis(2-methylpropionitrile) (AIBN), were dissolved in appropriate solvents in a mole ratio of 100:1:0.1, respectively, according to previously reported procedures. [2–4] The amount of solvent was equal to the amount of monomer by weight. The reaction mixture was degassed by nitrogen purge for 30 minutes. The reaction flask was sealed tightly with a rubber septum and heated in an oil bath at 75°C for the required time.

Synthesis of PS Macro-CTA

The synthesis of polystyrene (PS) macro-CTA follows the polymerization reaction procedure described above at 100°C with the following: monomer: styrene (S) (120.00 g, 1152.18 mmol); solvent: toluene (120.00 mL); precursor: CTA (2.82 g, 11.52 mmol); initiator: none; reaction time: 48 hours. The resulting polymer was precipitated dropwise into methanol and then redissolved in THF three times for purification. It was filtered and vacuum-dried to produce a pale-yellow powder (yield = 54%).

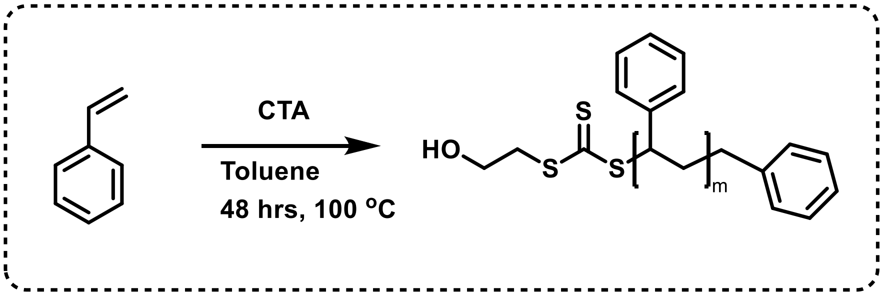

Scheme S2. Synthesis of PS Macro-CTA.

Synthesis of Poly(S-*b*-VBC)

The synthesis of Poly(S-*b*-VBC) (polystyrene-*block*-vinyl benzyl chloride) follows the polymerization reaction procedure described above at 75°C with the following: monomer: vinyl benzyl chloride (VBC) (20.25 g,199.00 mmol); solvent: THF (21.00 mL); precursor: PS macro-CTA (15.00 g, 1.99 mmol); initiator: AIBN (21.73 mg, 0.2 mmol); reaction time: 16 hours. The resulting polymer was precipitated dropwise in methanol and redissolved in THF three times for purification. It was filtered and vacuum-dried to produce a white powder (yield = 28%).

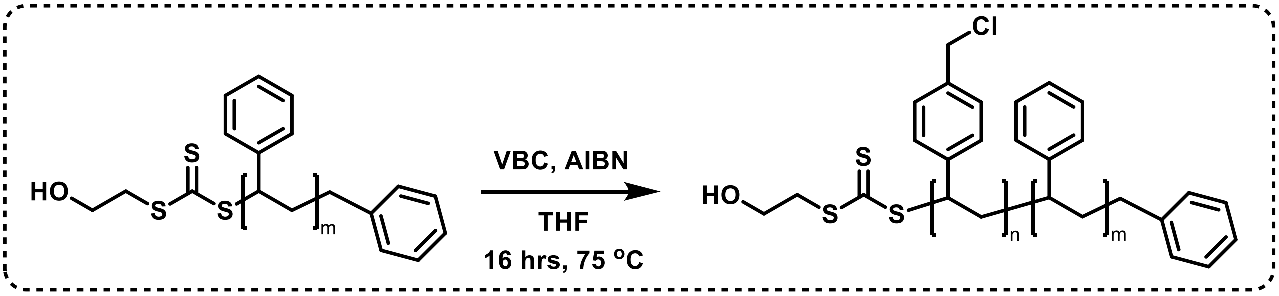

Scheme S3. Synthesis of Poly(S-*b*-VBC)

Synthesis of Poly(S-*b*-VBC-*b*-HA)

The synthesis of Poly(S-*b*-VBC-*b*-HA) (polystyrene-*block*-vinyl benzyl methyl imidazolium chloride-*block*-hexyl acrylate) follows the polymerization reaction procedure described above at 75°C with the following: monomer: hexyl acrylate (HA) (1.00 g, 6.00 mmol); solvent: THF (1.00 mL); precursor: poly(S-*b*-VBC) (1.00 g, 0.06 mmol); initiator: AIBN (1.00 mg, 0.006 mmol); reaction time: 6 hours. The resulting polymer was precipitated dropwise into hexane and then redissolved in THF three times for purification. It was filtered and vacuum-dried to produce a white powder (yield = 20%).

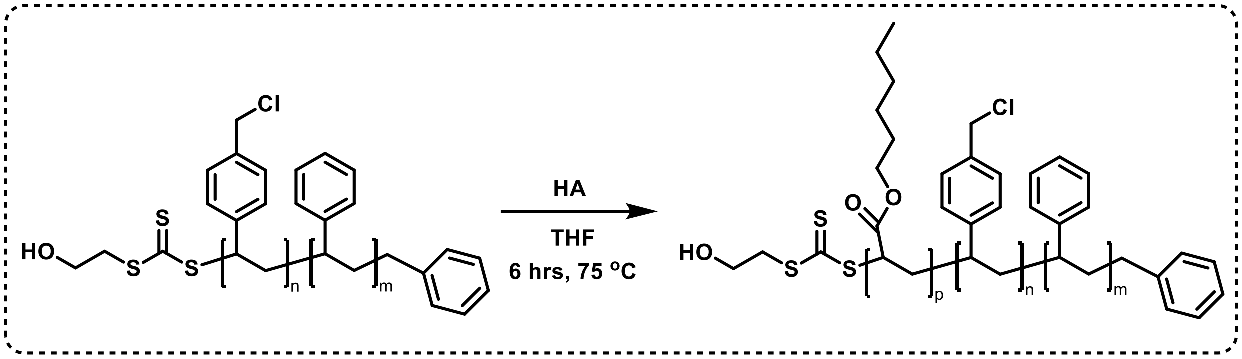

Scheme S4. Synthesis of Poly(S-*b*-VBC-*b*-HA)

Synthesis of Poly(S-*b*-VBMIm-Cl-*b*-HA)

Poly(S-*b*-VBMIm-Cl-*b*-HA) (polystyrene-*block*-vinyl benzyl methyl imidazolium chloride-*block*-hexyl acrylate) was synthesized from poly (S-*b*-VBC-*b*-HA) (1.50 g, 0.050 mmol) and 1-methylimidazole (0.62 g, 7.50 mmol) dissolved in DMF (6.00 mL) in a sealed round-bottom flask. The sealed flask was then placed into an oil bath at 80°C and stirred for 48 hrs. The resulting polymer was precipitated into about 20 mL of hexane and decanted (10 times). It was then filtered and vacuum-dried to produce an orange-colored powder (yield = 91%).

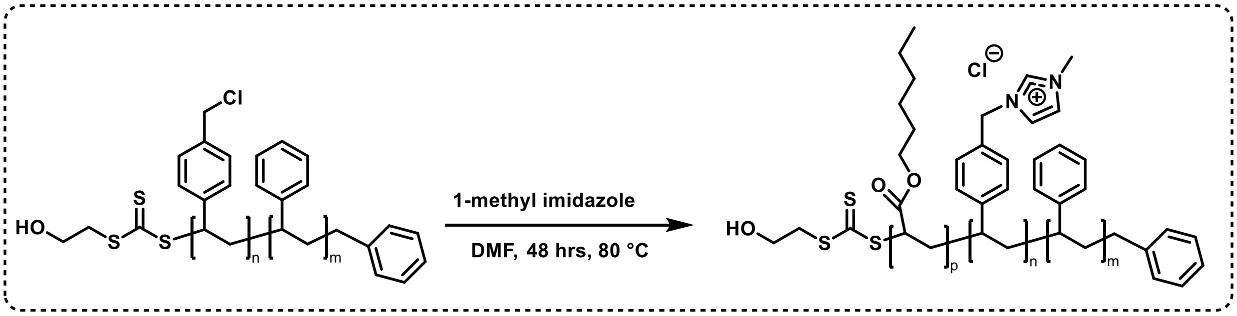

Scheme S5. Synthesis of Poly(S-*b*-VBMIm-Cl-*b*-HA)

XB Assembly Sample Preparation

Stock solutions of the XB-acceptor polymer **P** (2 mmol) and additives (240 mmol); pentafluoroiodobenzene (**PFIB**), nonafluoro-1-iodobutane (**NFIB**), and hexafluorobenzene (**HFB**) were prepared in methylene chloride. Samples for analysis were prepared by diluting stock solutions to obtain three stoichiometric mixtures of 1:1, 1:2, and 1:4 binding equivalents (Cl^- to I atoms) of **P** to additives. Each assembly mixture was kept in an airtight container and stirred overnight to form XB assemblies. For solid-state measurements, samples were drop-cast onto a glass plate, and the solvent was allowed to evaporate at room temperature. The solid samples were then isolated for measurements.

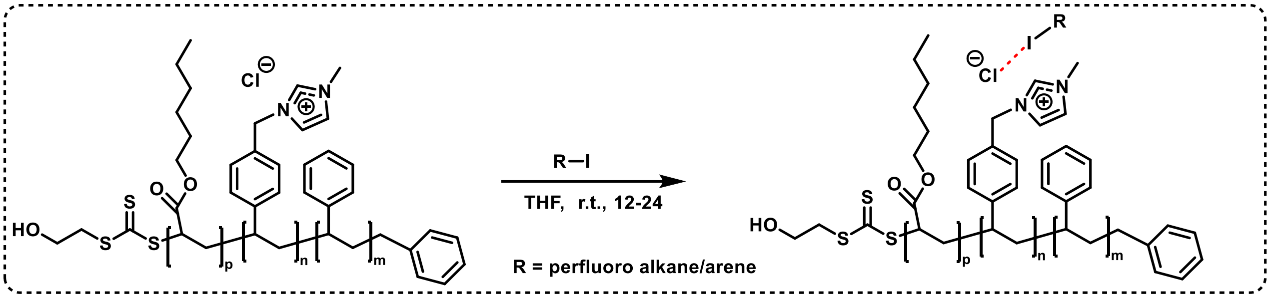

Scheme S6. Synthesis of XB Assemblies

3. Instrumentation and Results

Gel Permeation Chromatography (GPC)

Degrees of polymerization and dispersity of the synthesized polymers were determined using a Shimadzu HPLC system equipped with an autosampler, a heated column compartment, with a refractive index detector (RID). The column is a KF-805L GPC column from Shodex and is calibrated from 1 kDa to 1 MDa. The system was operated at 1 mL/min. Samples (1 mg/mL) were run in THF at 40 ^oC using polystyrene standards as reference.

Table S1. GPC characterization of synthesized polymers: Mn(g/mol): molecular number estimated from GPC analysis, DP: degree of polymerization calculated based on Mn, Đ: dispersity determined based on the GPC measurements.

Polymer	**Mn (g/mol)**	**DP**	**Đ**
PS Macro-CTA	6015	55	1.23
Poly(S-*b*-VBC)	10432	30	1.20
Poly(S-*b*-VBC *b*-HA)	14292	25	1.39

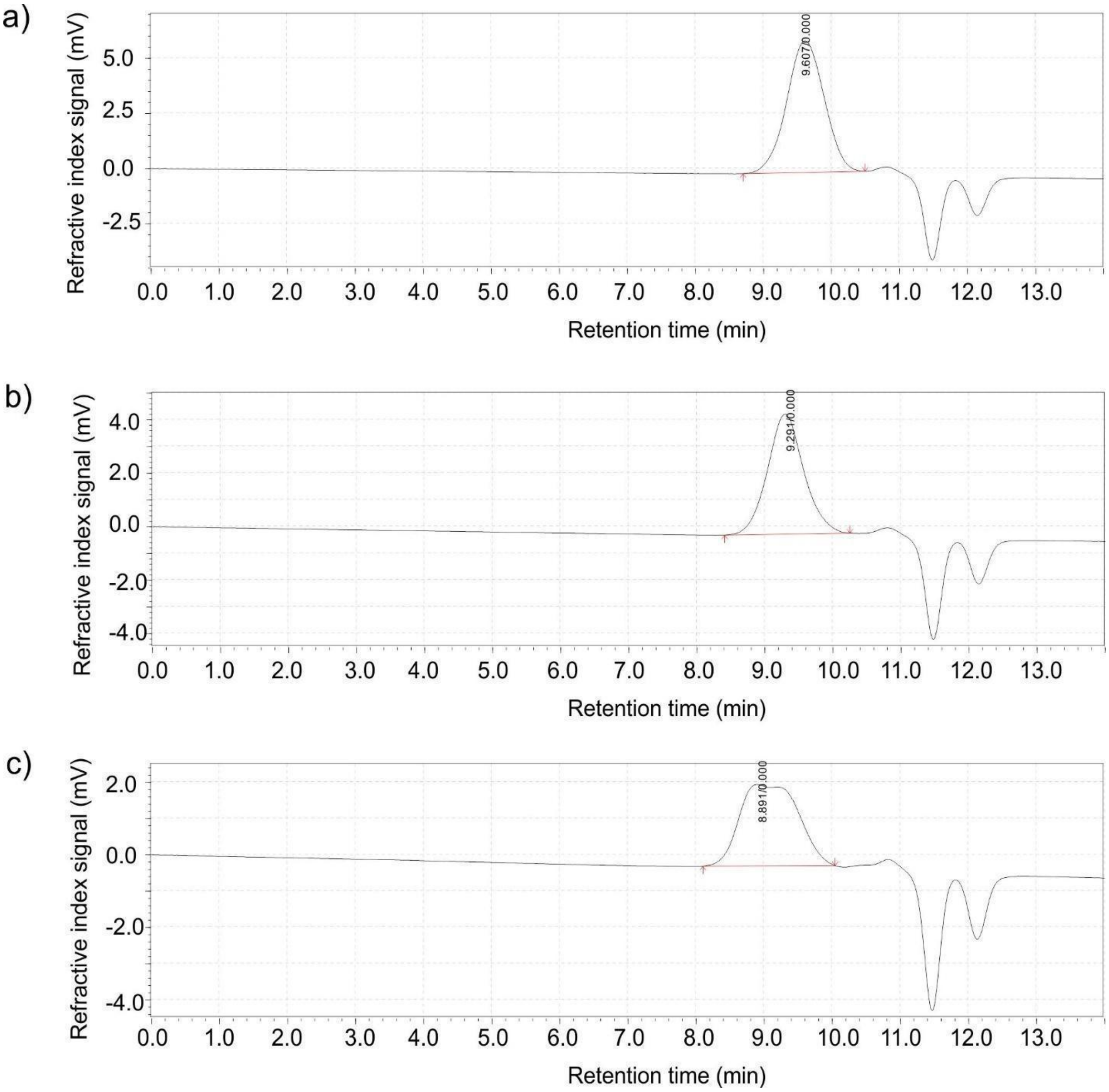

Figure S1. GPC Refractive Index chromatograms of: a) PS Macro-CTA, b) Poly(S-*b*-VBC), c) Poly(S-*b*-VBC *b*-HA)

Nuclear Magnetic Resonance (NMR)

^{1}H and ^{19}F NMR were done to confirm the synthesis of precursors and polymers, and to confirm XB interactions, respectively. Spectra were recorded with a Bruker Avance 400 instrument using deuterated solvents at 273K. For the ^{1}H measurements, the residual solvent peak was used as an internal standard. For the ^{19}F spectra, trifluoroacetic acid (δ -76.00 ppm, CF_3COOH) was used as an external standard for peak calibration according to previously reported procedures.[5] Samples for ^{19}F were prepared according to XB-assembly sample preparation procedures as indicated above, using a polymer concentration of 2 mmol in CD_2Cl_2. All spectra were baseline and phase corrected.

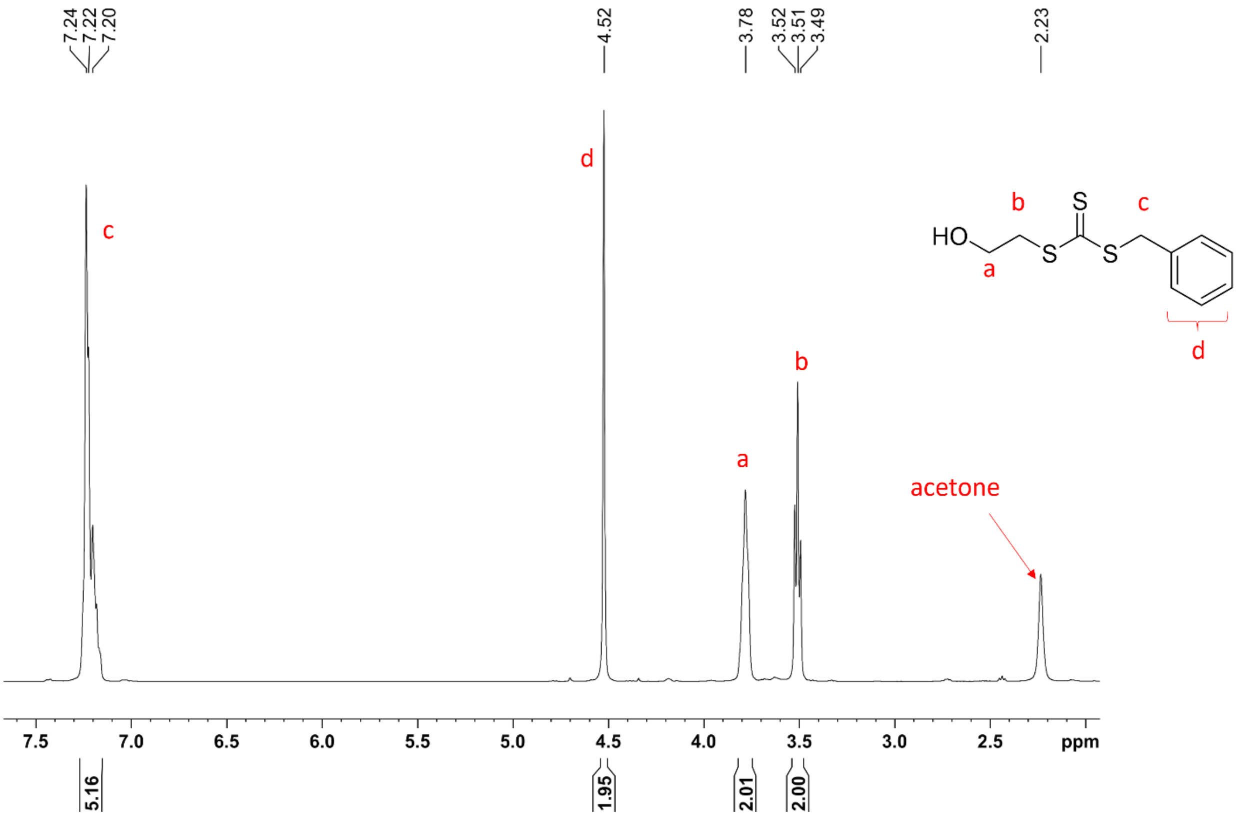

Figure S2. ^{1}H NMR of CTA in $CDCl_3$ at 298 K with peak assignments.

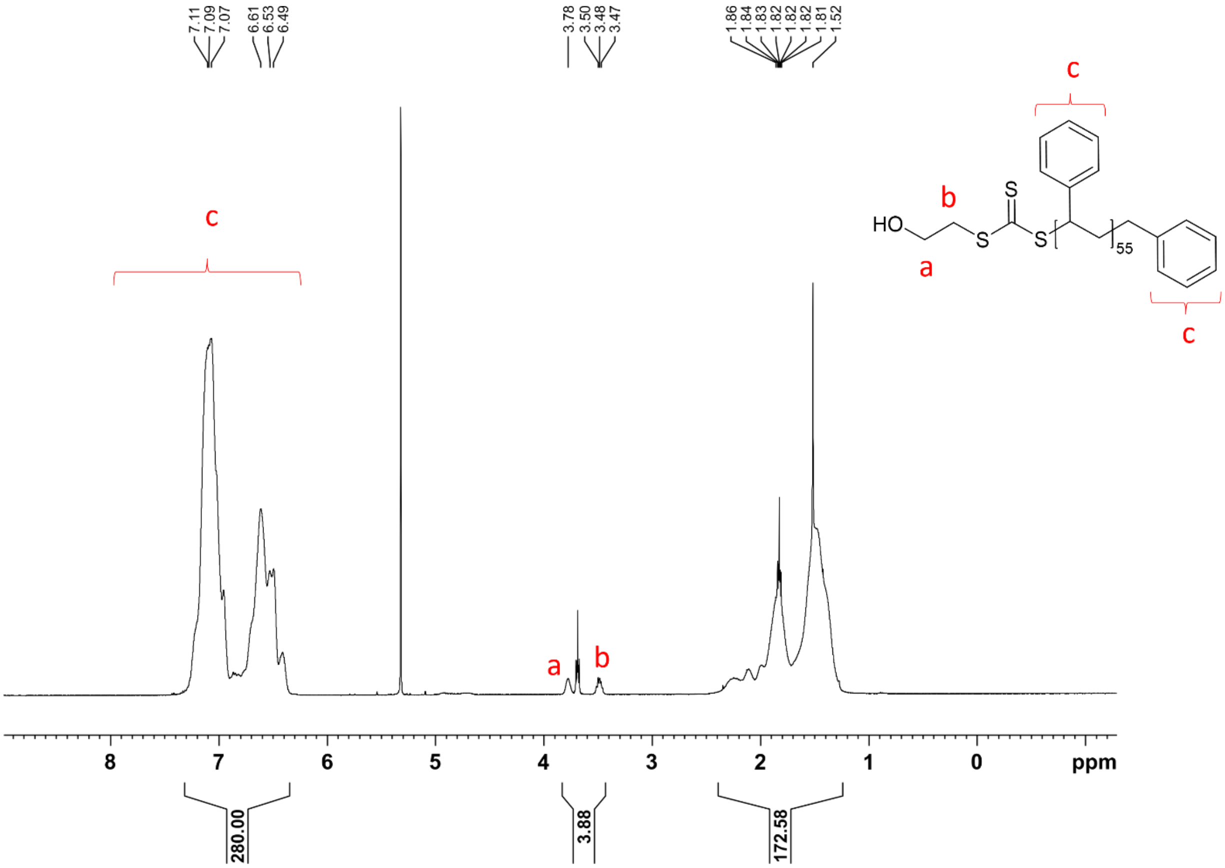

Figure S3. ^{1}H NMR of PS Macro-CTA in CD_2Cl_2 at 298 K with peak assignments.

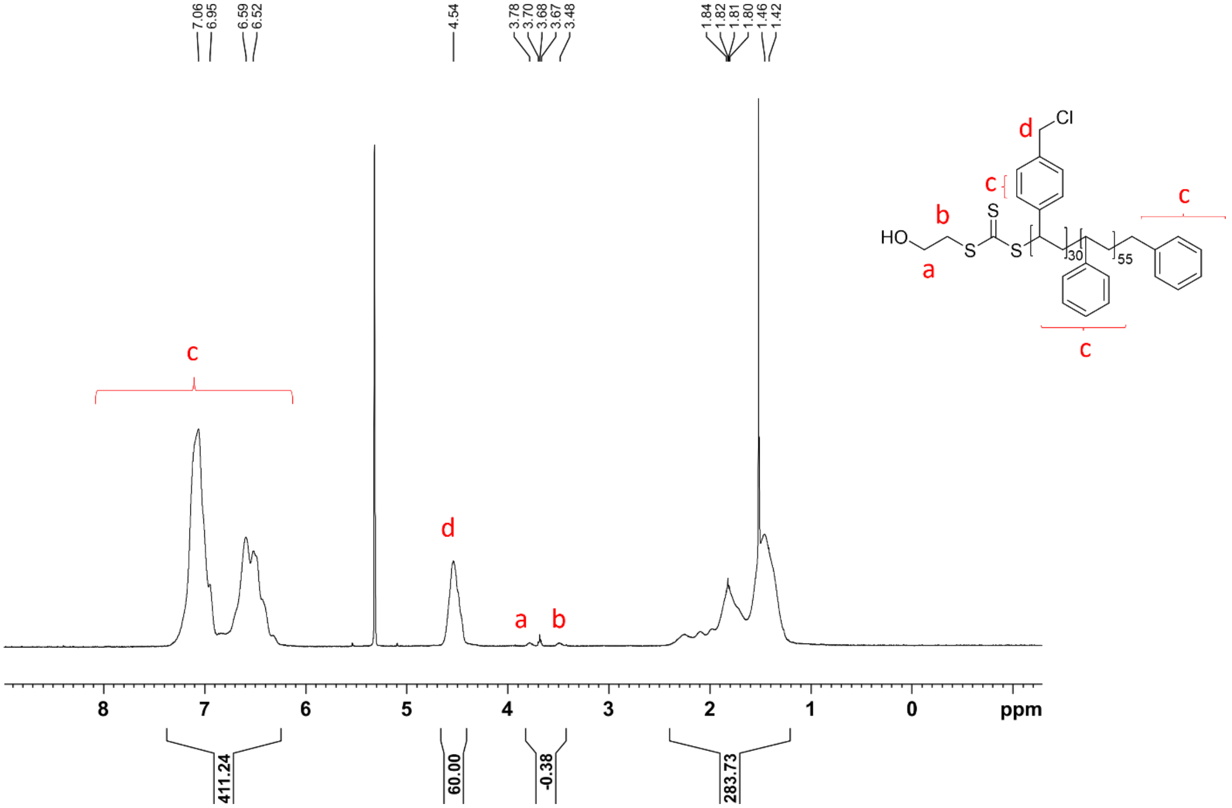

Figure S4. ^1H NMR of Poly(S-b-VBC) in CD_2Cl_2 at 298 K with peak assignments.

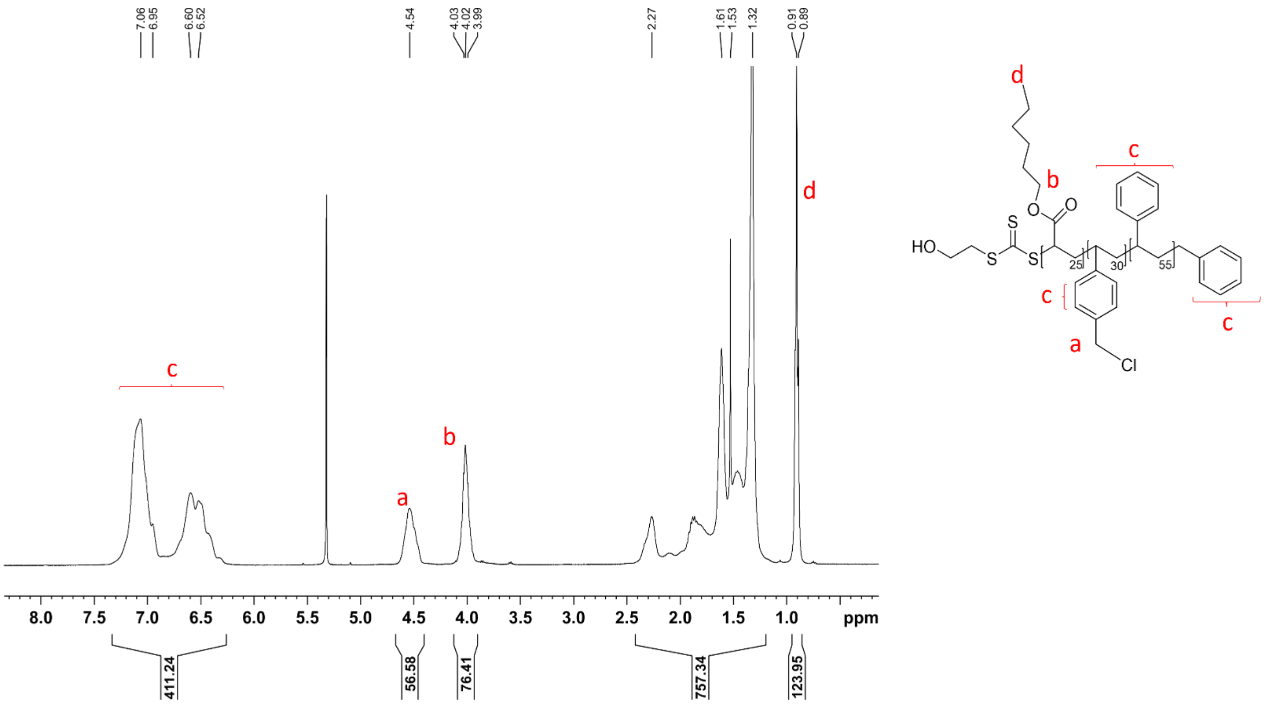

Figure S5. ^{1}H NMR of Poly(S-b-VBC-HA) in CD_2Cl_2 at 298 K with peak assignments.

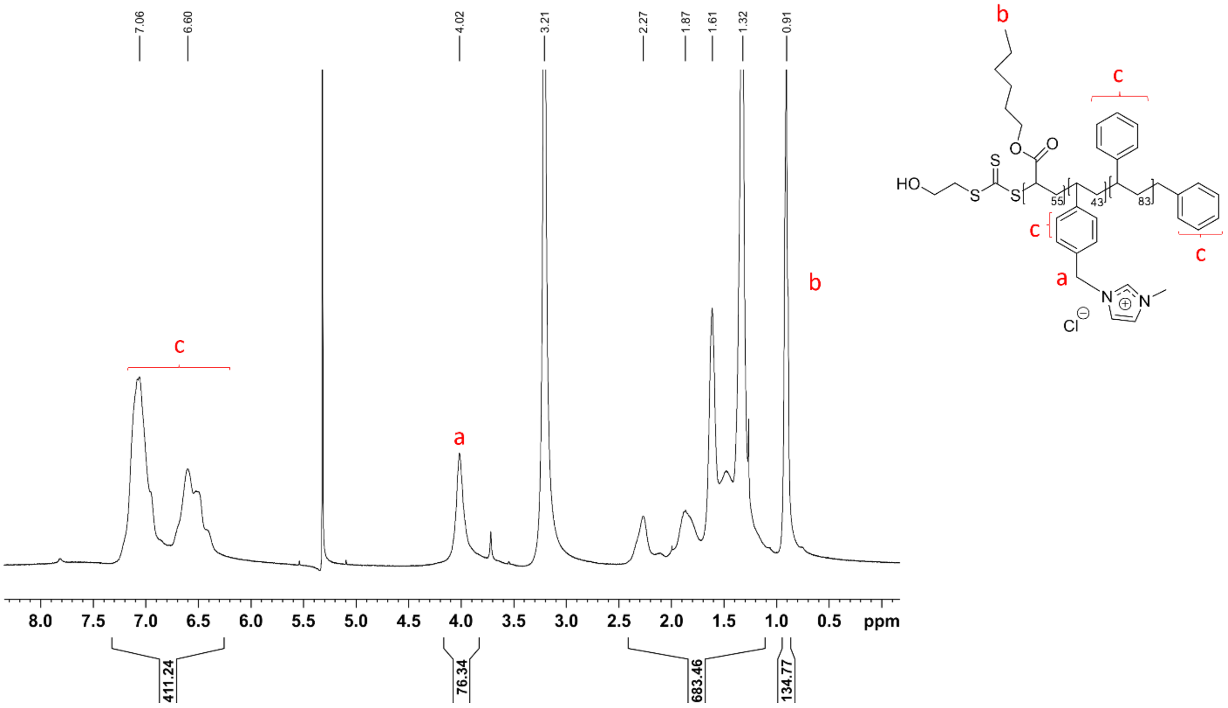

Figure S6. ^{1}H NMR of Poly(S-b-VBMImCl-HA) in CD_2Cl_2 at 298K with peak assignments

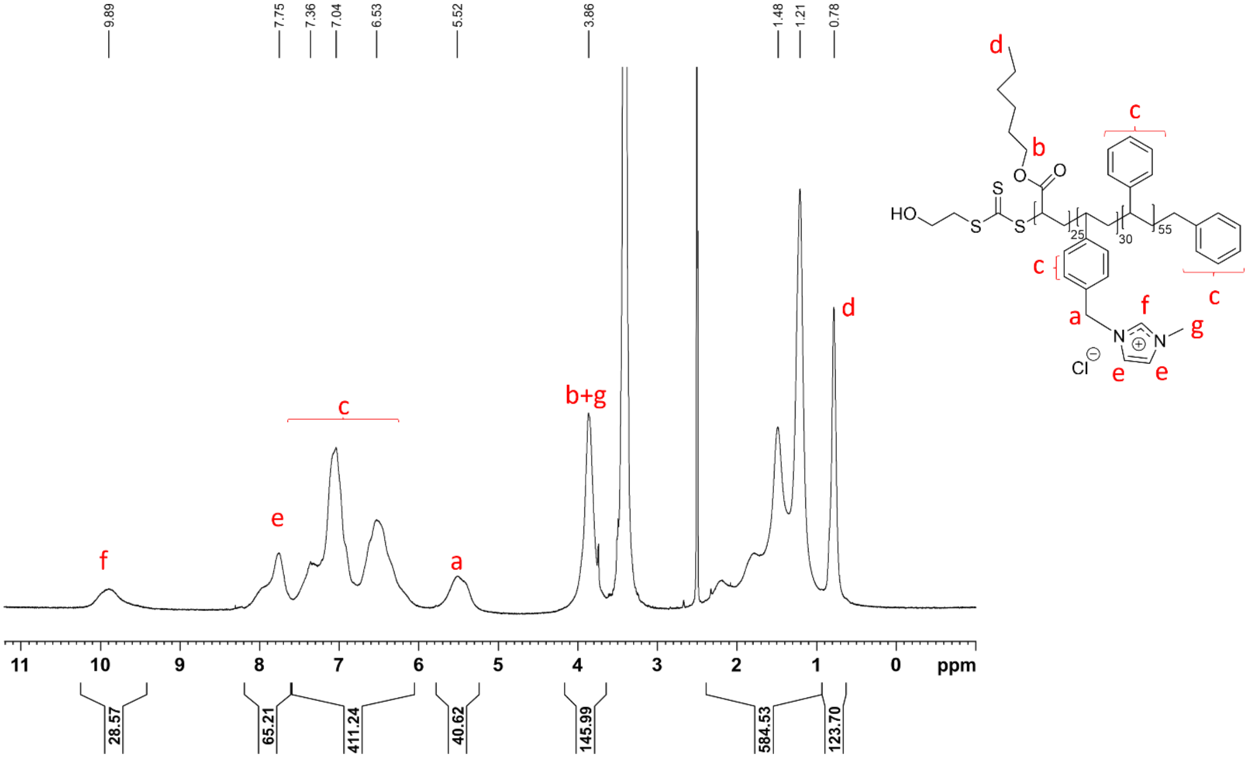

Figure S7. ^{1}H NMR of Poly(S-b-VBMImCl-HA) in DMSO-d_6 at 298K with peak assignments.

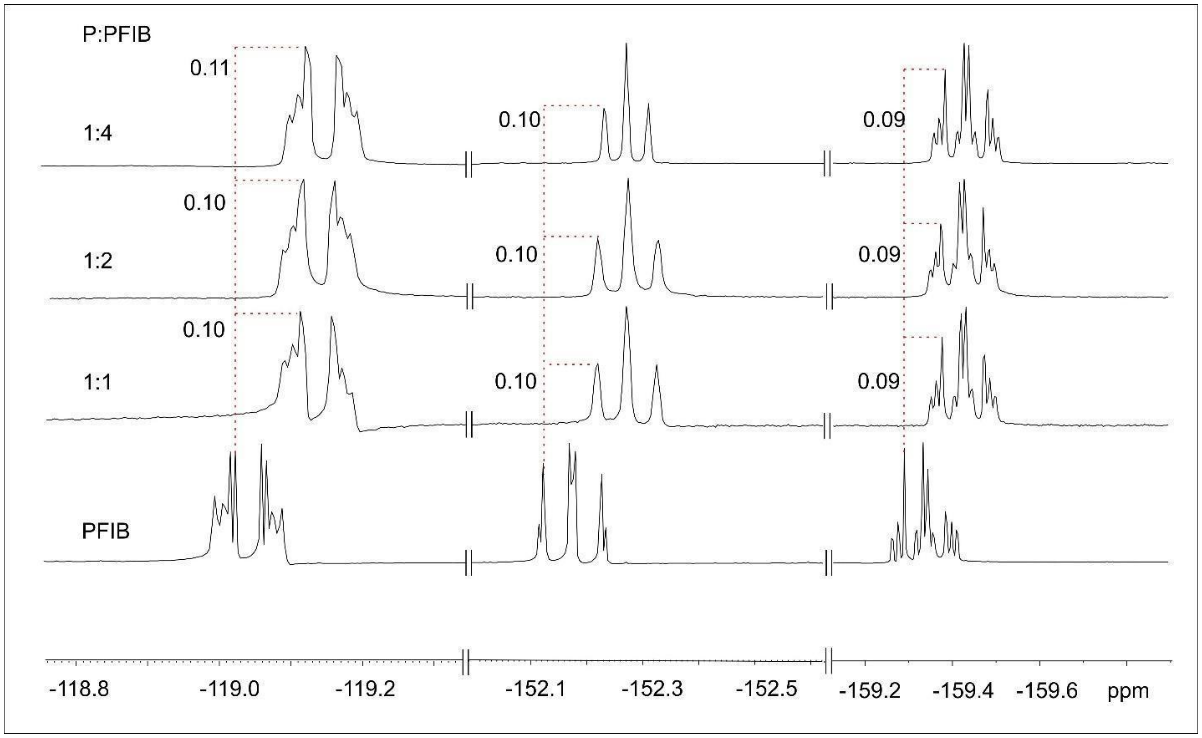

Figure S8. Sections of the ^{19}F NMR spectra (in CD_2Cl_2 at 298 K) of **PFIB** and **P–PFIB** ratios showing changes in chemical shifts relative to trifluoroacetic acid (δ -76.00 ppm, CF_3COOH).

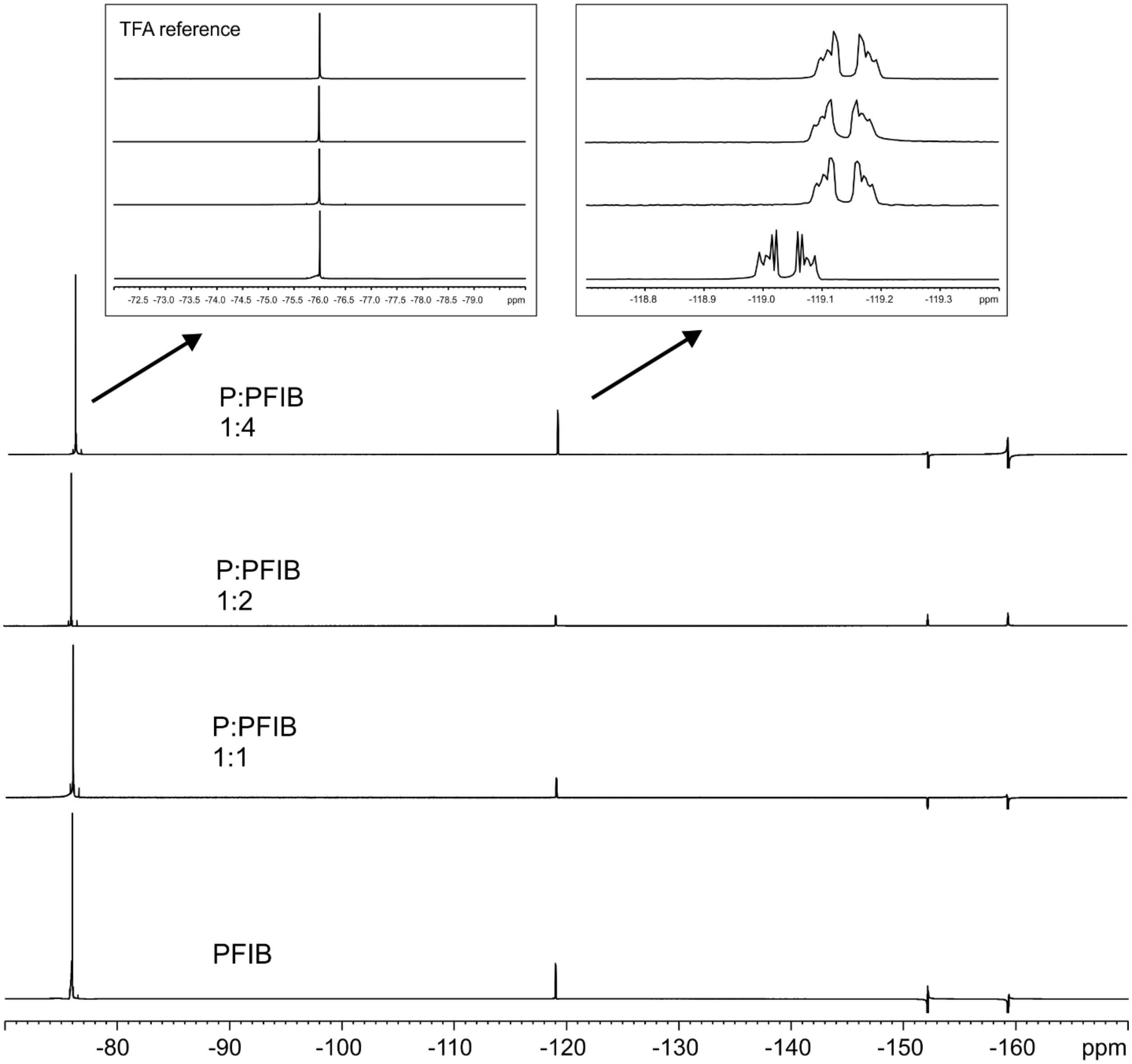

Figure S9. Full spectra of the ^{19}F NMR (in CD_2Cl_2 at 298 K) of **PFIB** and **P–PFIB**. Insets show the Trifluoroacetic acid (TFA) reference and the fluorine signal closest to the iodine on **PFIB**.

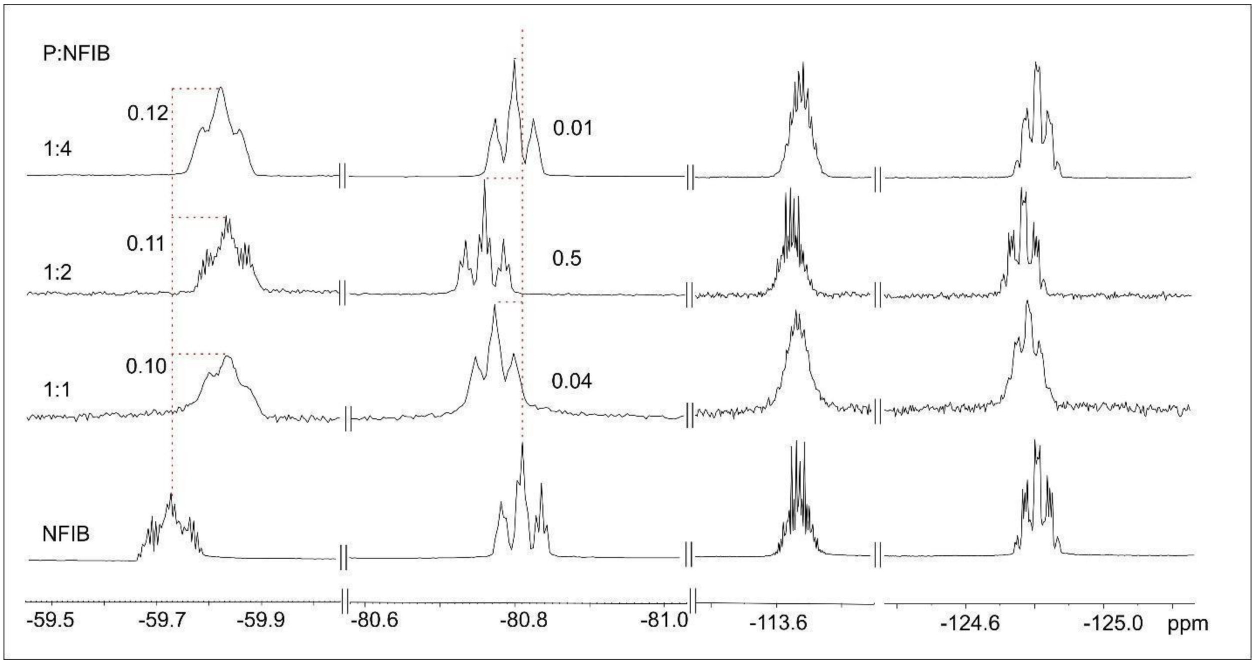

Figure S10. Sections of the ^{19}F NMR spectra (in CD_2Cl_2 at 298 K) stack of **NFIB** and **P–NFIB** ratios, showing changes in chemical shifts, relative to trifluoroacetic acid (δ -76.00 ppm, CF_3COOH).

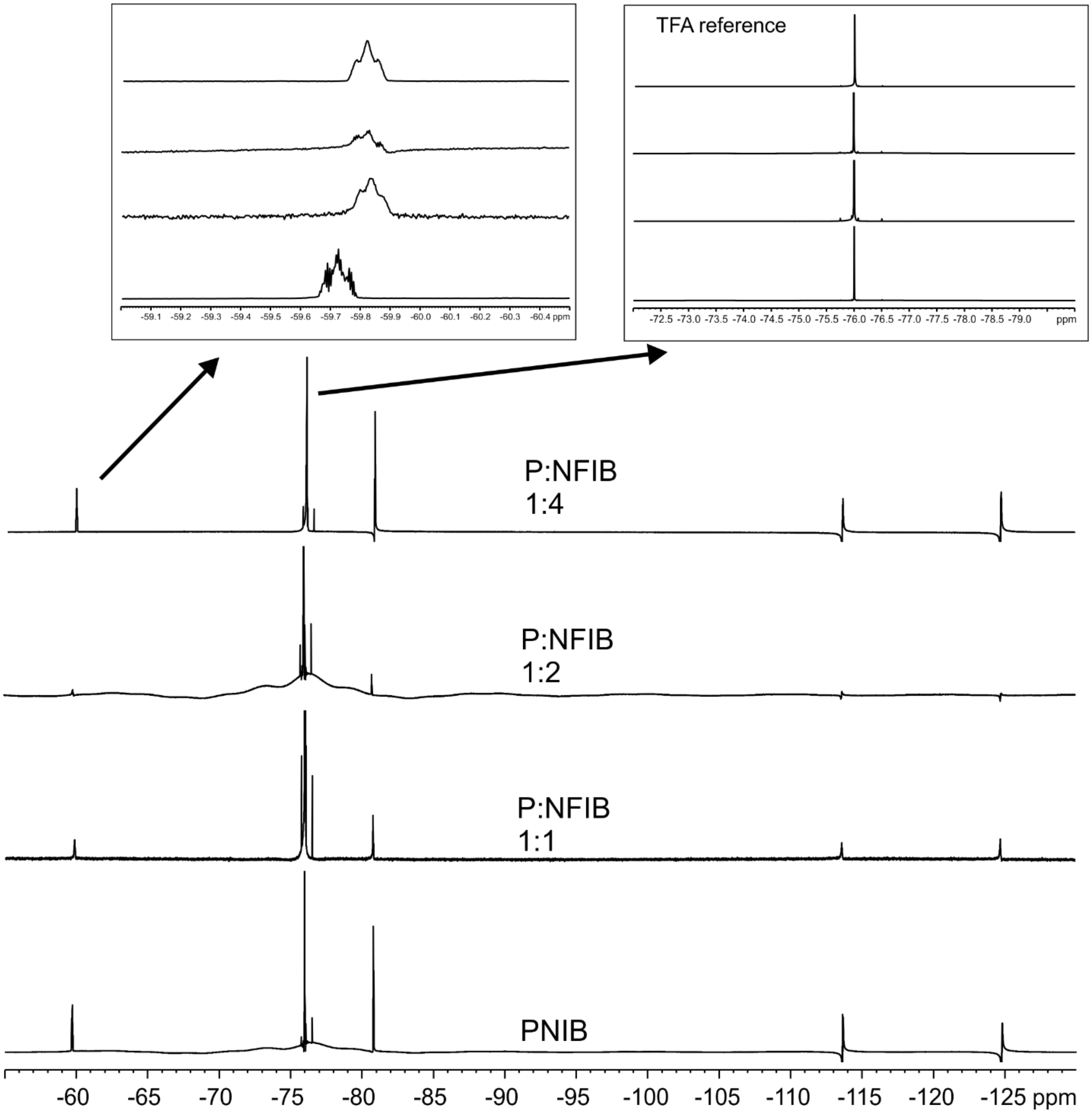

Figure S11. Full spectra of the ^{19}F NMR (in CD_2Cl_2 at 298 K) of **NFIB** and **P–NFIB**. Inserts show the Trifluoroacetic acid (TFA) reference and the fluorine signal closest to the iodine on **NFIB**.

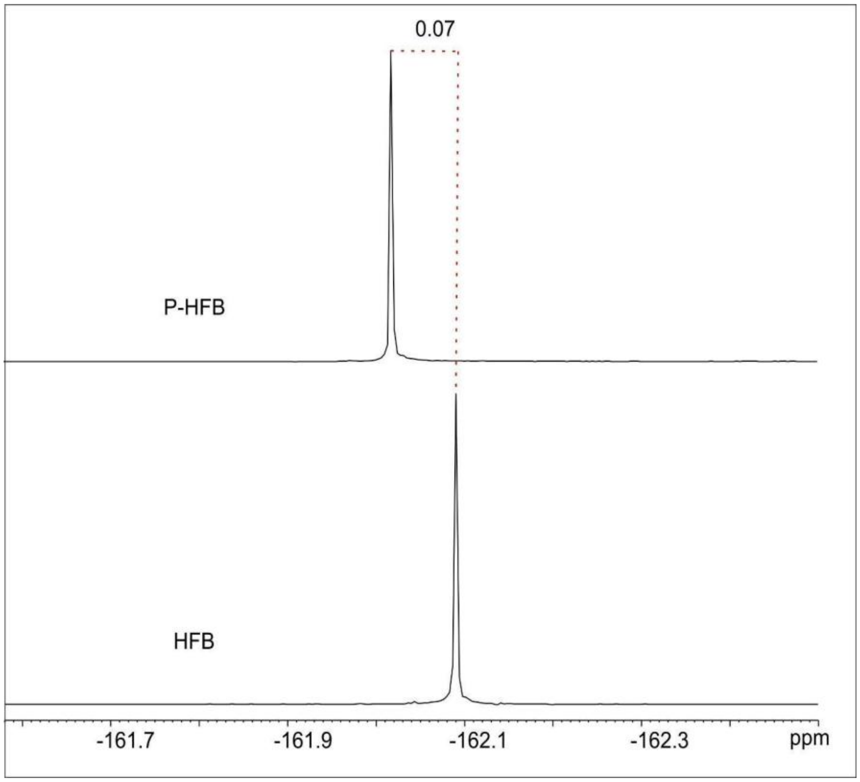

Figure S12. Sections of the ^{19}F NMR spectra (in CD_2Cl_2 at 298 K) stack of **HFB** and control **P–HFB** assembly, showing changes in chemical shifts.

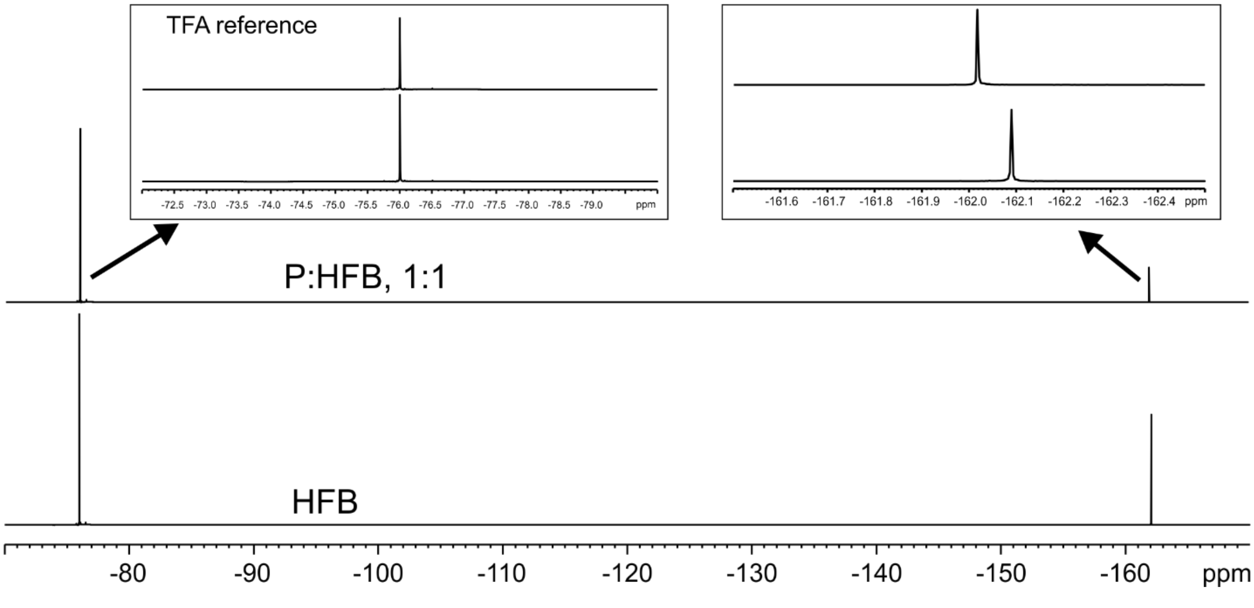

Figure S13. Full spectra of the ^{19}F NMR (in CD_2Cl_2 at 298 K) of **HFB** and **P–HFB**. Insets show the Trifluoroacetic acid (TFA) reference and the fluorine signal of **HFB**.

Fourier-transform infrared (FTIR)

FTIR spectra were measured on a Bruker Alpha FT-IR with a Platinum ATR Attachment. Measurements were conducted in transmission mode in mid-IR region (500-4000 cm^{-1}, resolution 4 cm^{-1}. Samples were prepared according to XB-assembly sample preparation procedures above, using a polymer concentration of 2mmol in methylene chloride. The obtained data were normalized to improve comparison and replotted with Excel.

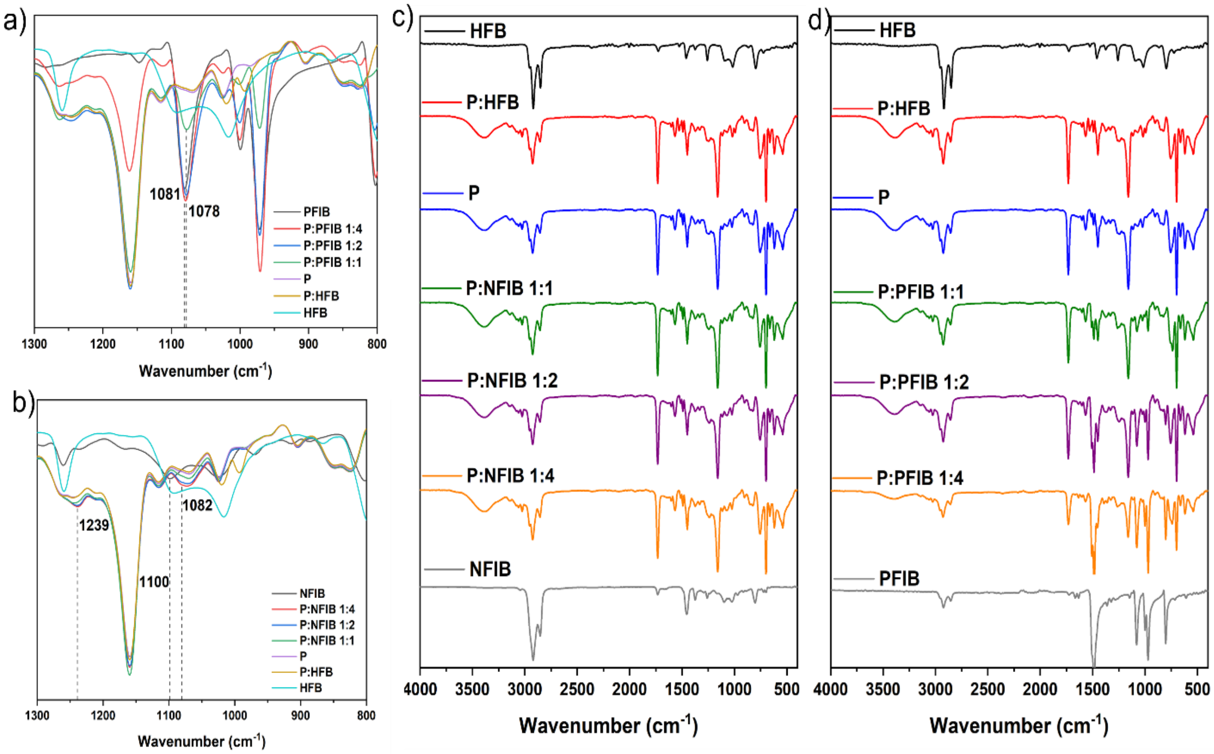

Figure S14. FTIR: a) partial spectra showing peak changes in **P–PFIB** assemblies. b) partial spectra showing peak changes in **P–NFIB** assemblies. c) full spectra showing **P**, **HFB**, **NFIB**, **P–NFIB**, and **P–HFB** assemblies. d) full spectra showing **P**, **HFB**, **PFIB**, **P–PFIB**, and **P–HFB** assemblies.

Isothermal Titration Calorimetry (ITC)

The ITC experiment was carried out by filling the sample cell with the polymer, **P**, (0.1 mM in CH_2Cl_2), filling the syringe with either **HFB**, **NFIB**, or **PFIB** (1 mM in CH_2Cl_2), and titrating via computer-automated injector at 298K. Blank titrations into plain CH_2Cl_2 solvent were also performed and subtracted from the corresponding titration to remove any effect from the heats of dilution from the titrant. Isotherms and thermodynamic parameters from a sequential binding model (Ka, ΔH, and ΔS) were obtained using the NaNoAnalyze software. Gibbs' free energy ΔG was subsequently calculated at 298K and recorded. The data were fitted to a two-site and three-site sequential binding model.

Table S2: Thermodynamic parameters associated with the binding of the polymer, **P**, by the components **PFIB**, **NFIB**, and **HFB** in CH_2Cl_2 at 298K. K_d in µM, *ΔH* in kJ/mol, *TΔS* in kJ/mol, and *ΔG* in kJ/mol.

P-HFB	K_{d1}	8.296 ±2.824E-13	ΔH_1	1.004E3 ±5.734E1	$T\Delta S_1$	1.032E3	ΔG_1	-28.000
	K_{d2}	1.576 ±9.136E-15	ΔH_2	-5.255E2 ±6.201E1	$T\Delta S_2$	-4.920E2	ΔG_2	-35.300
P-PFIB	K_{d1}	1.955 ±2.853E2	ΔH_1	-4.536 ±7.708E1	$T\Delta S_1$	2.80E1	ΔG_1	-32.546
	K_{d2}	9.984E4 ±5.561E4	ΔH_2	4.465E2 ±5.064E3	$T\Delta S_2$	4.521E2	ΔG_2	-5.600
	K_{d3}	8.589E4 ±7.253E4	ΔH_3	-1.951E3 ±3.172E3	$T\Delta S_3$	-1.944E3	ΔG_3	-7.000
P-NFIB	K_{d1}	1.000E5 ±2.866E4	ΔH_1	7.391E3 ±6.489E3	$T\Delta S_1$	7.393E3	ΔG_1	-2.000
	K_{d2}	1.000E5 ±3.101E4	ΔH_2	-5.000E3 ±5.394E3	$T\Delta S_2$	-4.992E3	ΔG_2	-8.000
	K_{d3}	1.000E-4 ±2.230E-18	ΔH_3	-2.500E3 ±3.375E3	$T\Delta S_3$	-2.442E3	ΔG_3	-58.000

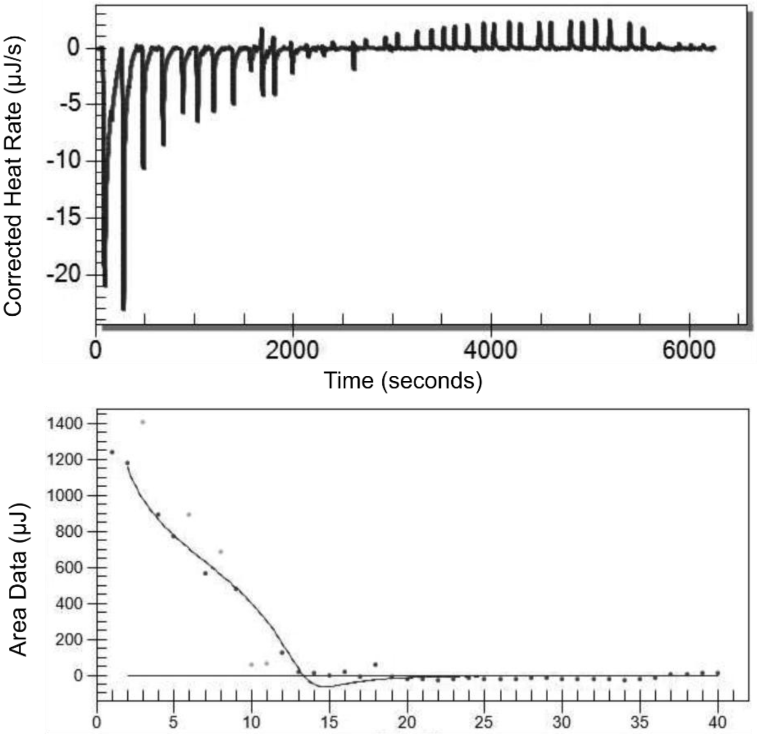

Figure S15. ITC traces of the titration into P with HFB in CH_2Cl_2 at 298K. The data were fitted into a two-site sequential binding model.

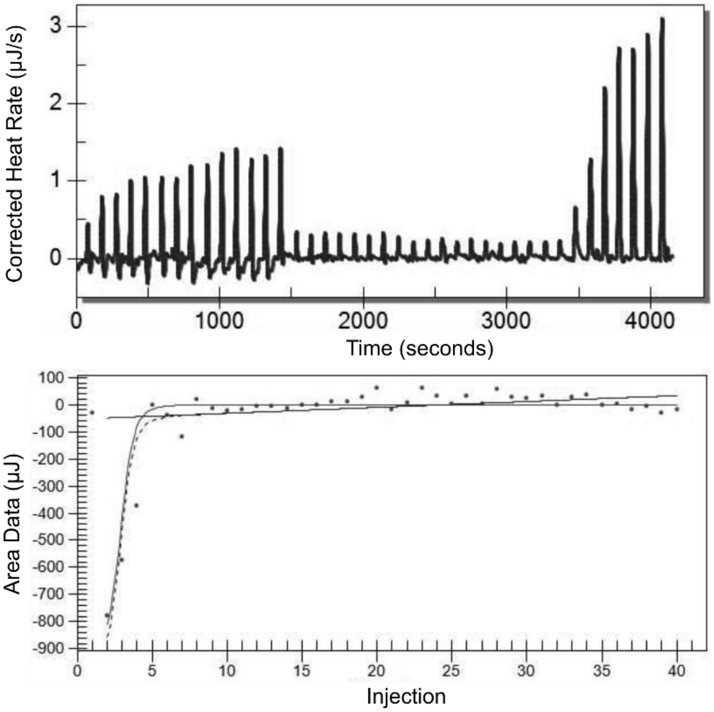

Figure S16. ITC traces of the titration into P with NIFB in CH_2Cl_2 at 298K. The data were fitted into a three-site sequential binding model.

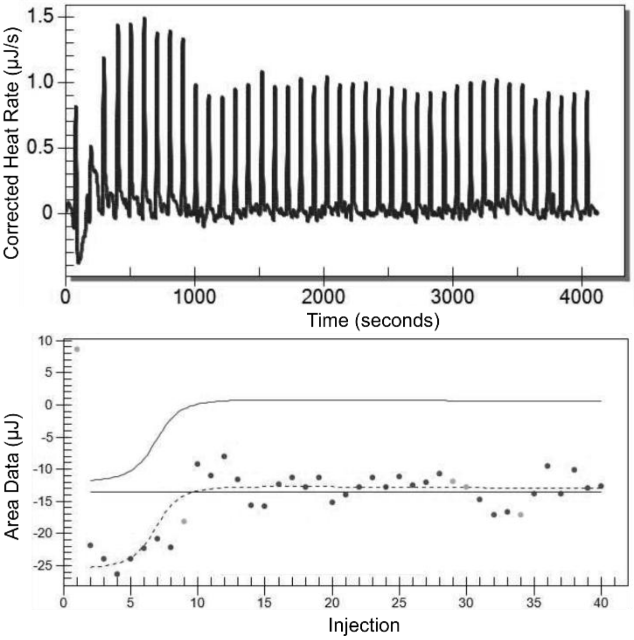

Figure S17. ITC traces of the titration into P with PIFB in CH_2Cl_2 at 298K. The data were fitted into a three-site sequential binding model.

Dynamic light scattering (DLS)

Intensity-size distributions, particle sizes, and polydispersity indices of the XB-donating polymer and XB assemblies were determined using Zetasizer Nano ZS device (Malvern Instruments) with a 4 mW He-Ne ion laser at the wavelength of 633 nm and an Avalanche photodiode detector at an angle of 173°. Samples were prepared according to XB-assembly sample preparation procedures above, using a polymer concentration of 10 µmol in methylene chloride. Samples were collected into quartz cuvettes for measurements. Each sample was measured three times, and the average results presented. Experiments were carried out at 20°C. Zetasizer software (Malvern Instruments) was used to obtain the data. Cumulant analysis gave the z-average values, polydispersity indices, and the intensity size distribution graphs of particles.

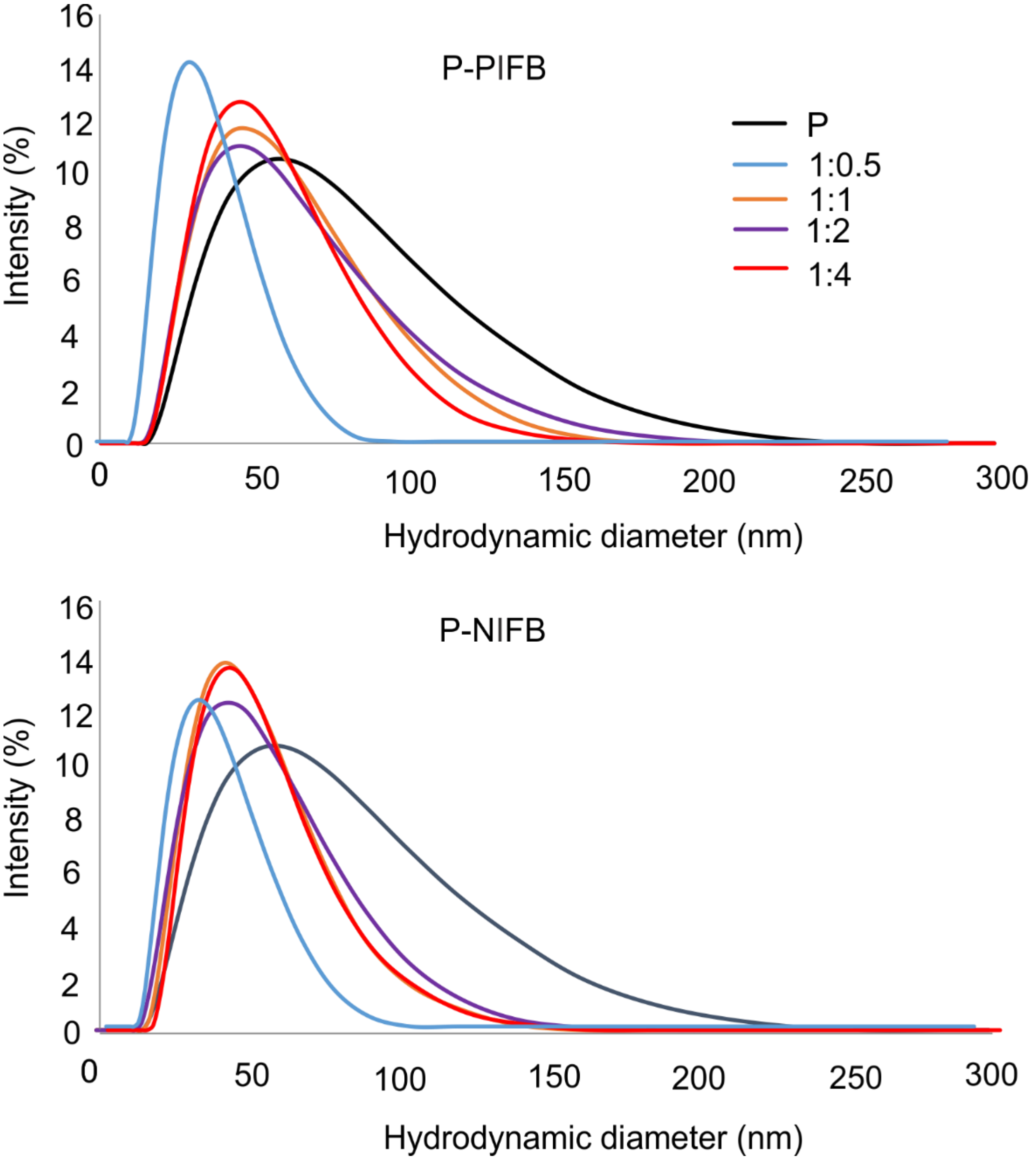

Figure S18. DLS intensity-size distribution curves of **P**, **P–PFIB**, and **P–NFIB** assemblies.

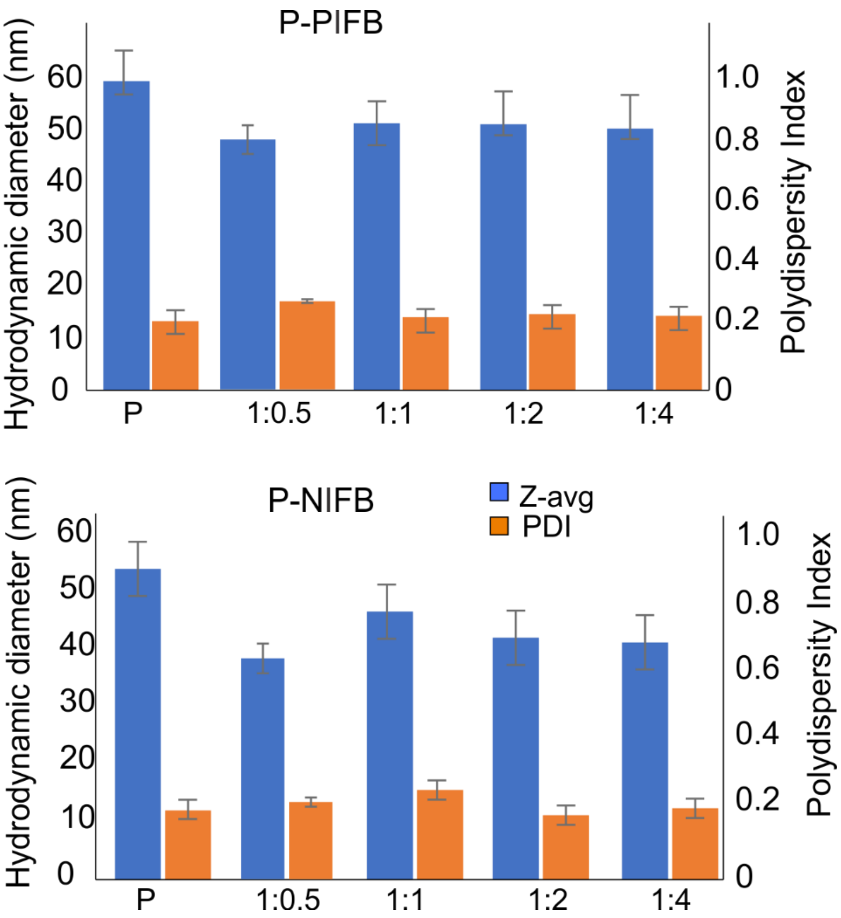

Figure S19. Bar graphs showing average hydrodynamic diameters and polydispersity indices of **P**, **P–PFIB**, and **P–NFIB** assemblies obtained from DLS measurements.

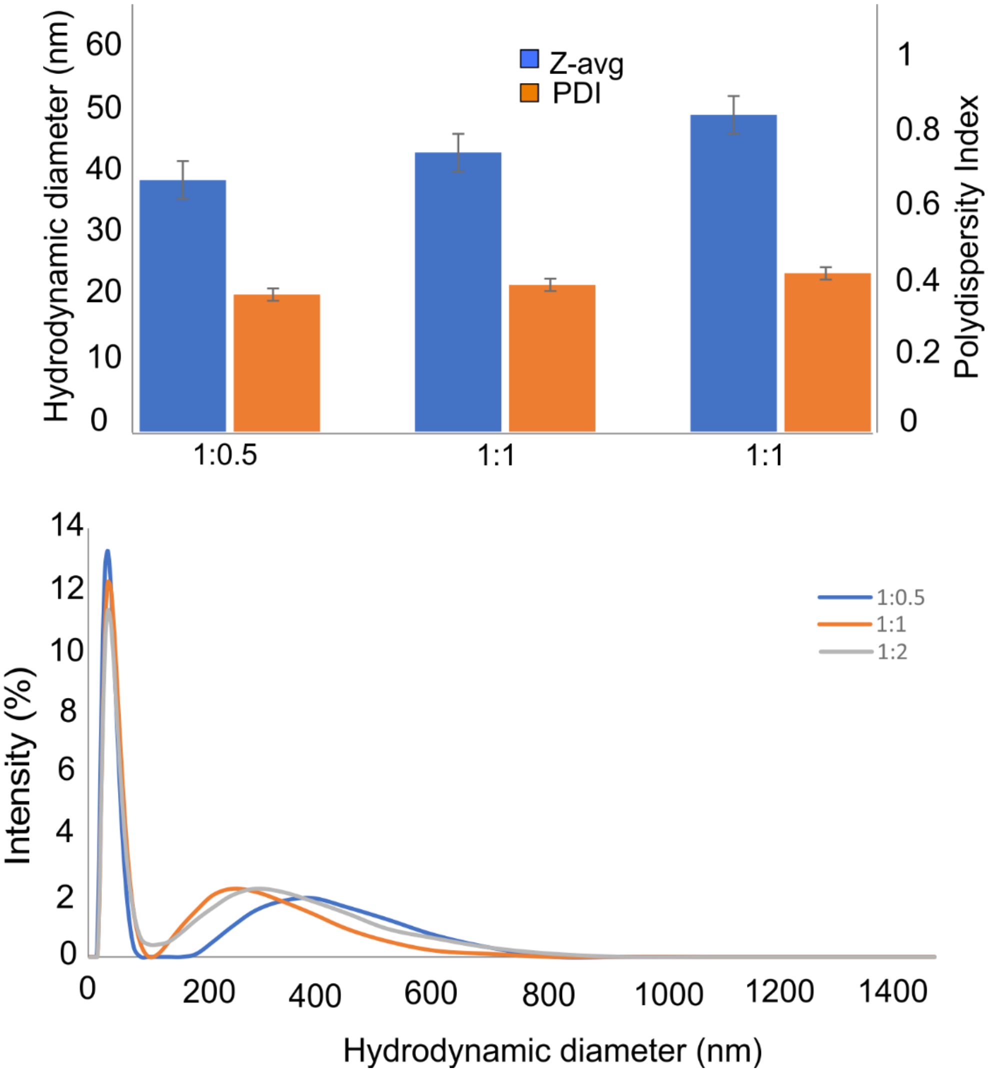

Figure S20. (Top) Bar graphs showing average hydrodynamic diameters and polydispersity indices, and (bottom) intensity-size distribution curves of control **P–HFB** assemblies obtained from DLS measurements.

Transmission electron microscopy (TEM)

The Talos F200X G2 S/TEM instrument was utilized for the TEM imaging at an acceleration voltage of 200 kV. Samples were prepared and measured right after DLS measurements. Samples were prepared on Formvar carbon-coated copper grids by adding 2 drops of the sample solutions to the grid. The sample drop was left on the grid for 1 min to dry. Finally, the samples were dried under ambient conditions for a minimum of 1 hour. TEM images were further analyzed with ImageJ program.

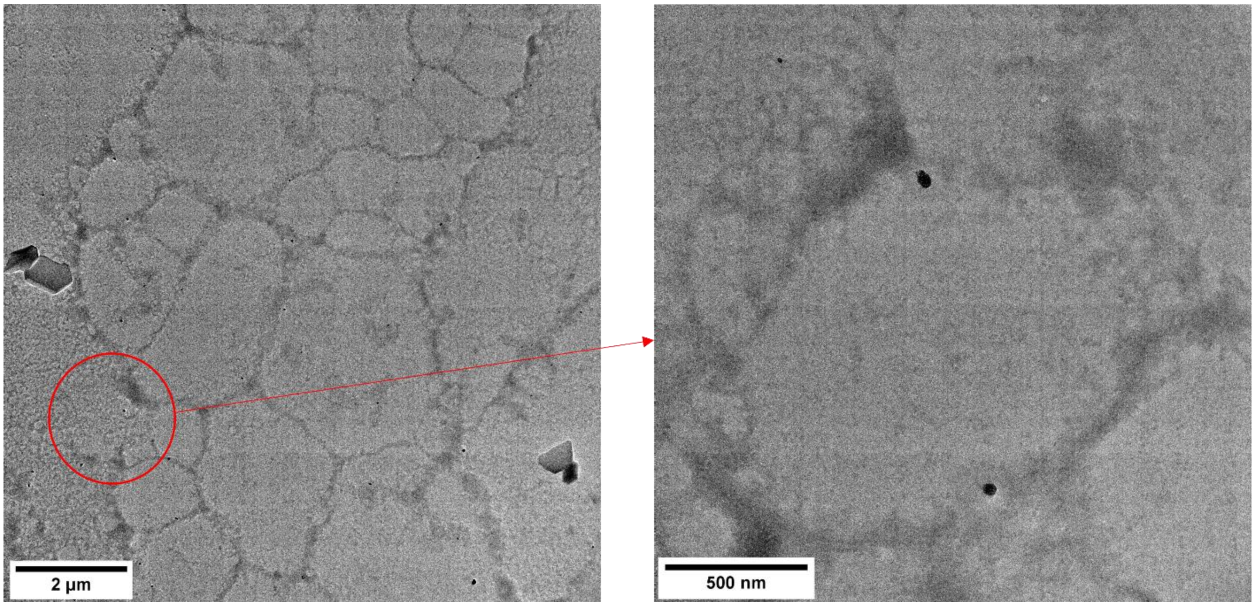

Figure S21. TEM images of Polymer **P**

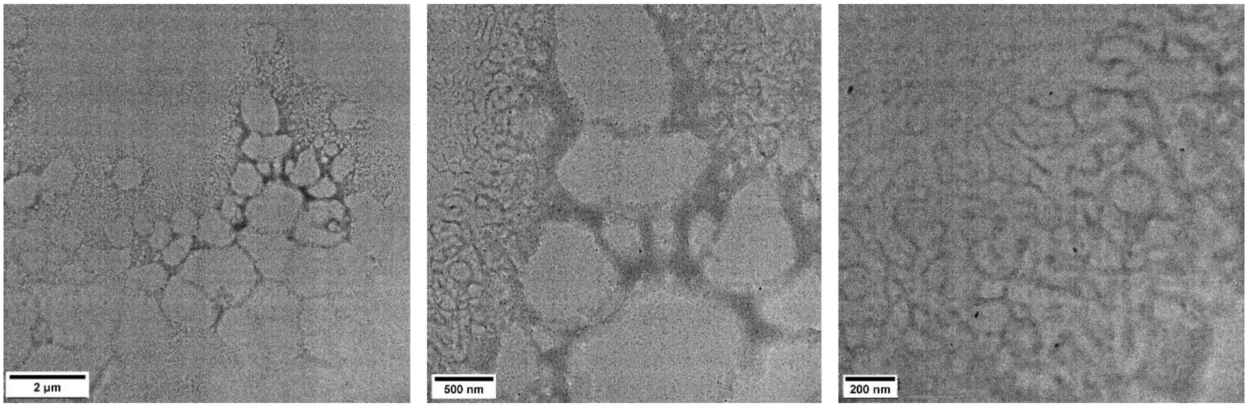

Figure S22. TEM images of the 1:1 ratio of **P–PFIB** assembly

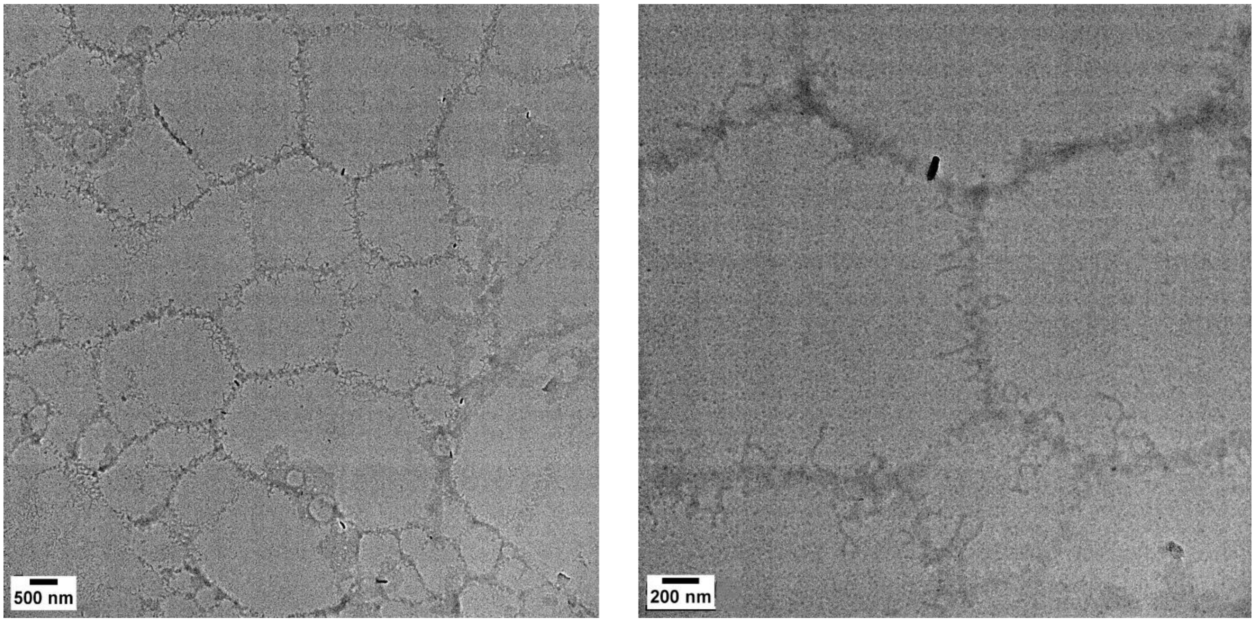

Figure S23. TEM images of the 1:2 ratio of **P–PFIB** assembly**.**

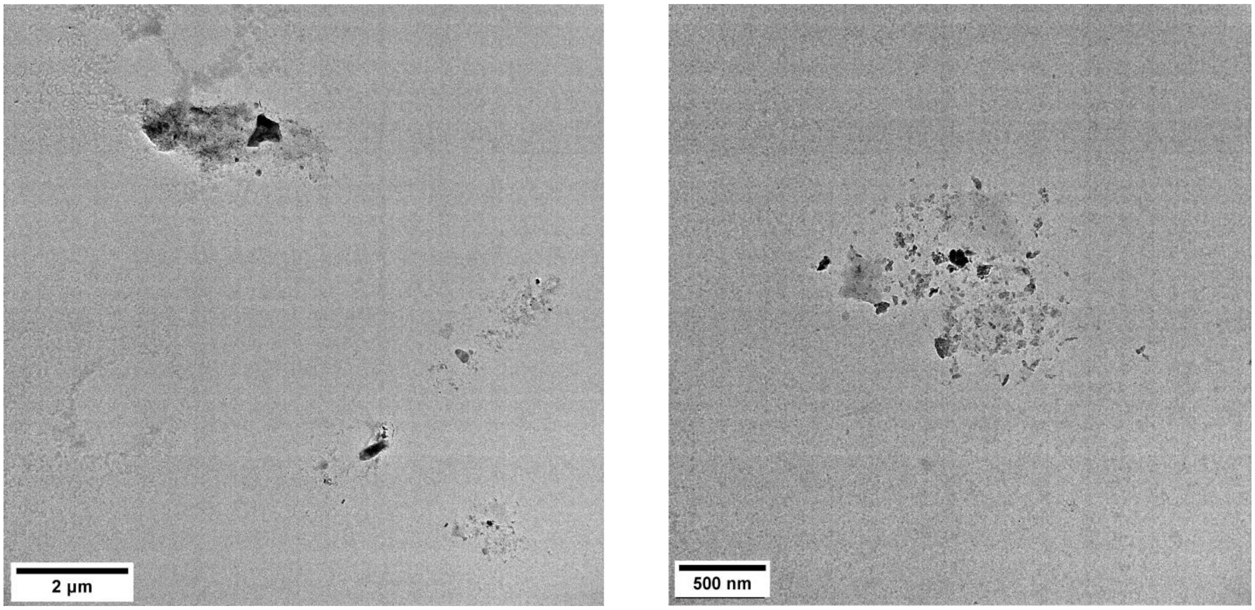

Figure S24. TEM images of the 1:4 ratio of **P–PFIB** assembly.

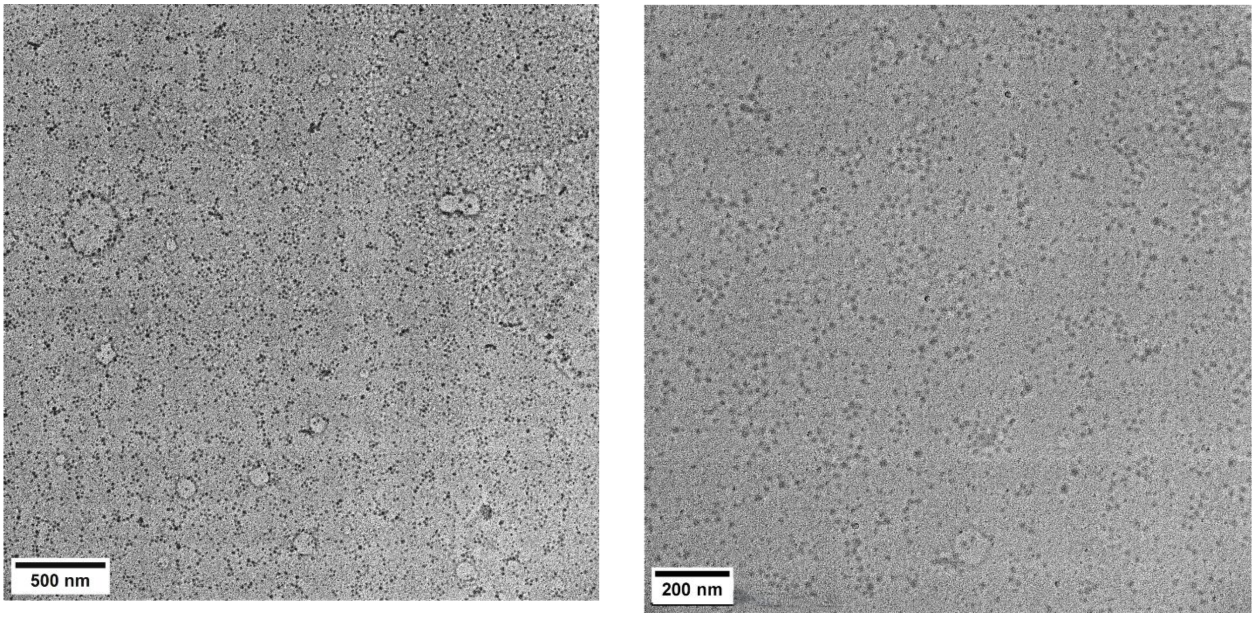

Figure S25. TEM images of the 1:1 ratio of **P–NFIB** assembly

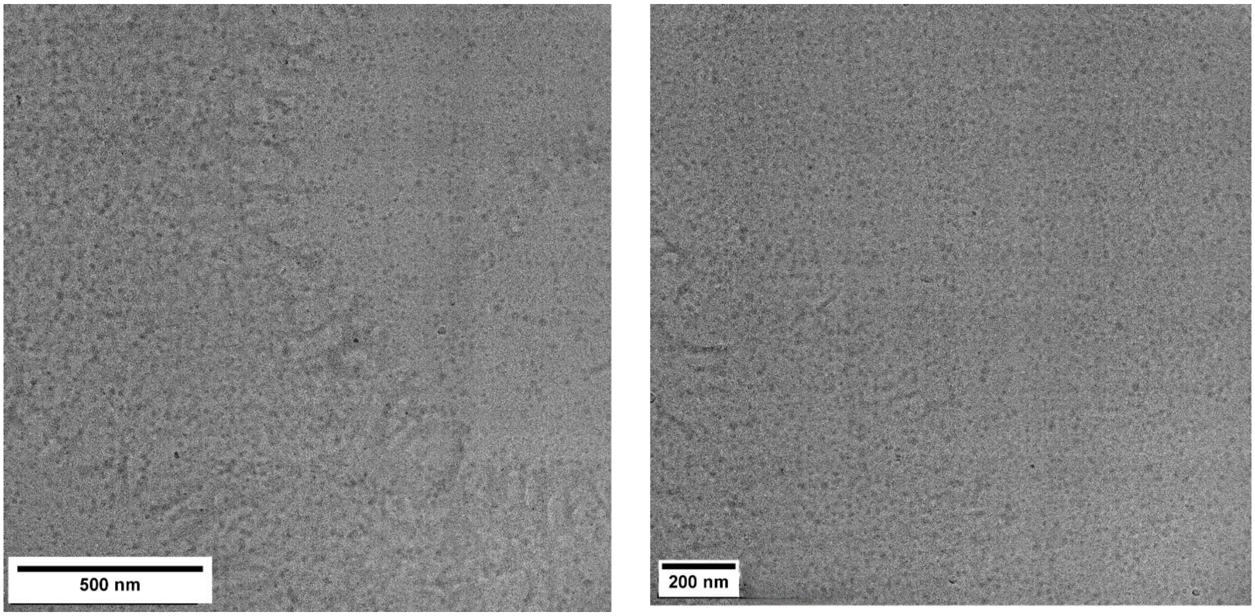

Figure S26. TEM images of the 1:2 ratio of **P–NFIB** assembly

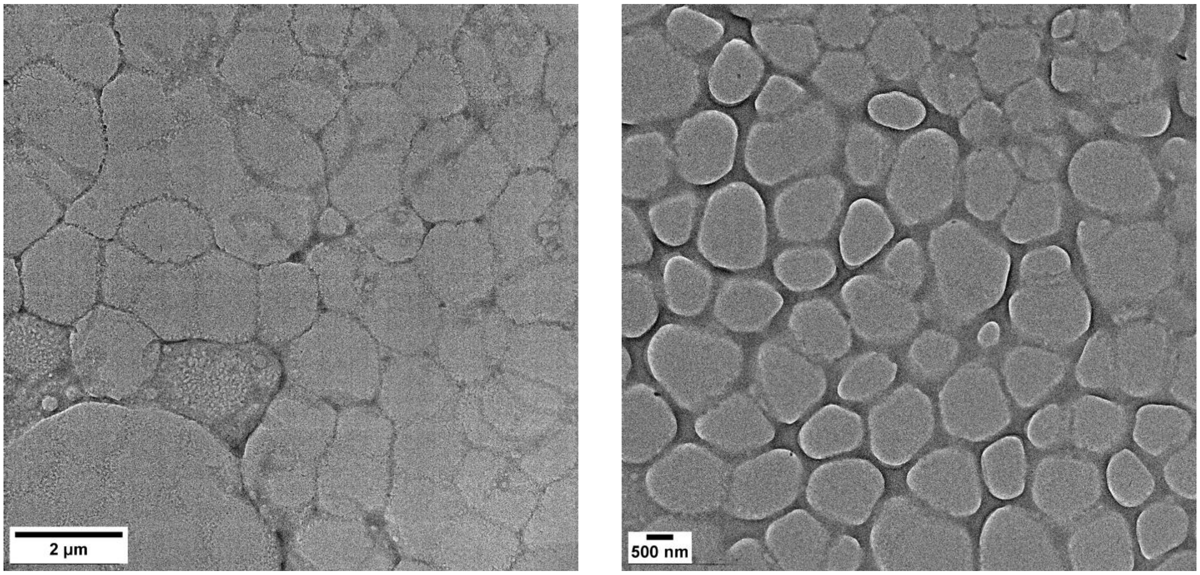

Figure S27. TEM images of the 1:4 ratio of **P–NFIB** assembly

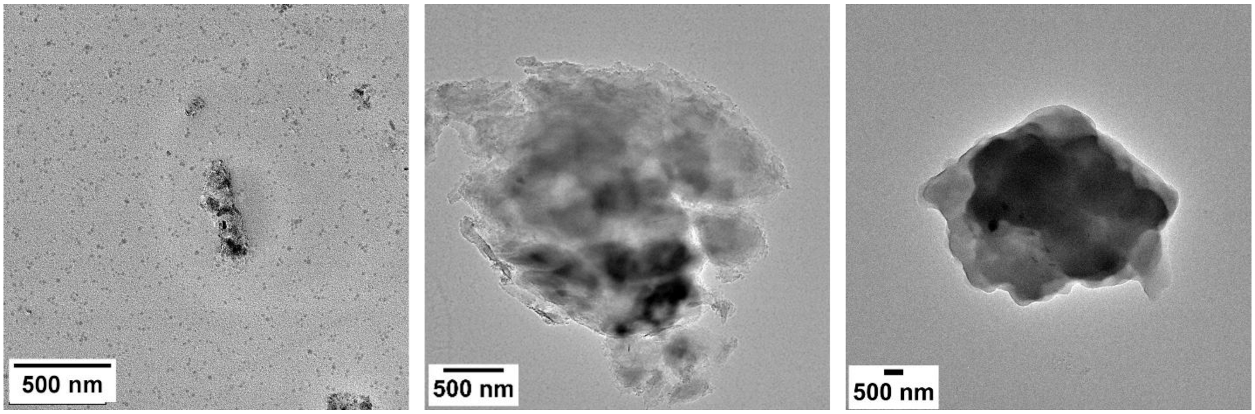

Figure S28. TEM images of the 1:0.5, 1:1, and 1:2 ratios of **P–HFB** assemblies.

Atomic Force Microscopy (AFM)

AFM was conducted using a Bruker Multi mode 8 AFM with a silicon cantilever (tap300IA-G) tip and a constant spring of 40 N/m. The scans were performed in air and in tapping mode, with a scan size of 20 µm × 20 µm at a scan rate between 0.5 - 0.8 Hz at 256 x 256 pixels. Before imaging, the sample was placed onto a metal disk containing a conductive adhesive carbon tape to hold it. The images were obtained by NanoScope Analysis and analyzed by Gwyddion, a software package for analyzing SPM data.

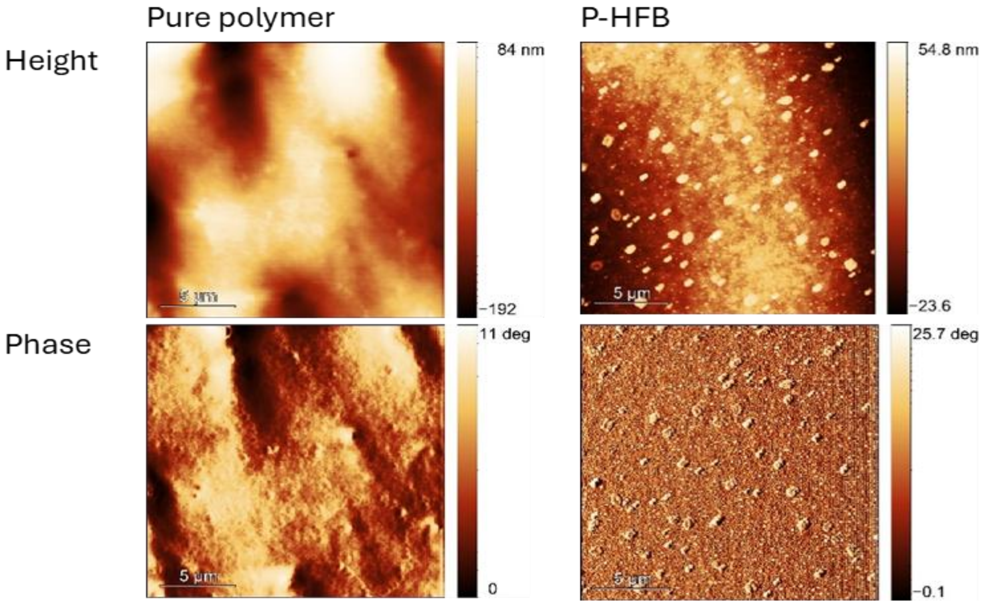

Figure S29. AFM phase and height images of **P** and control **P–HFB** assembly

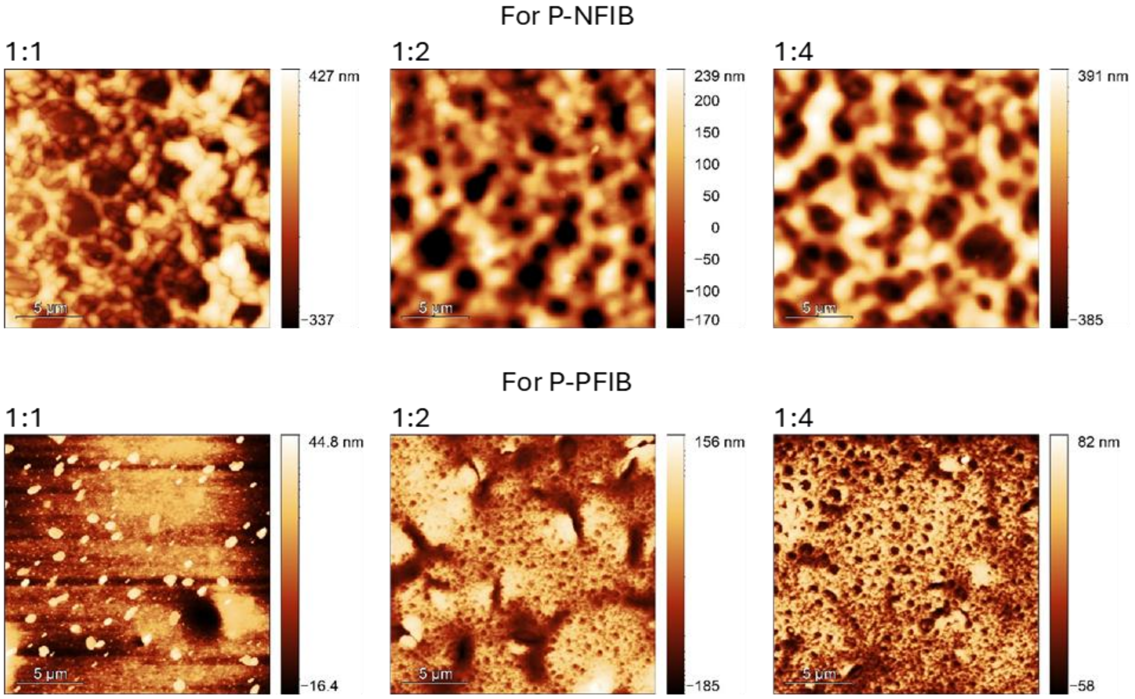

Figure S30. AFM height images of **P–NFIB** and **P–PFIB** assemblies.

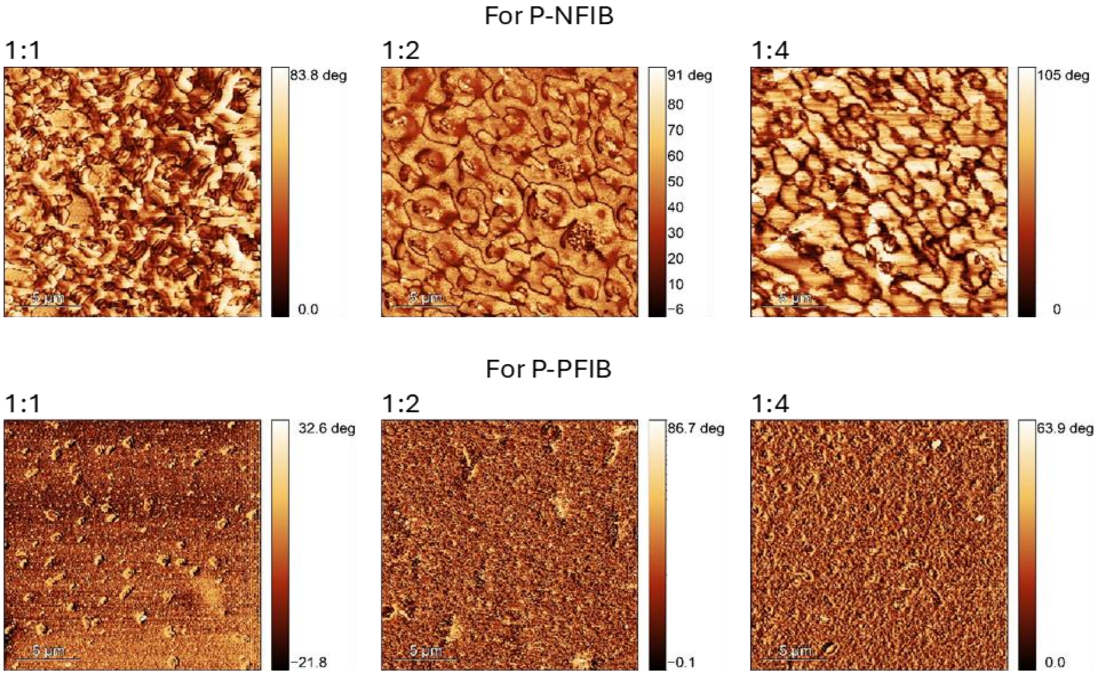

Figure S31. AFM phase images of **P–NFIB** and **P–PFIB** assemblies.

For P-NFIB 1:4

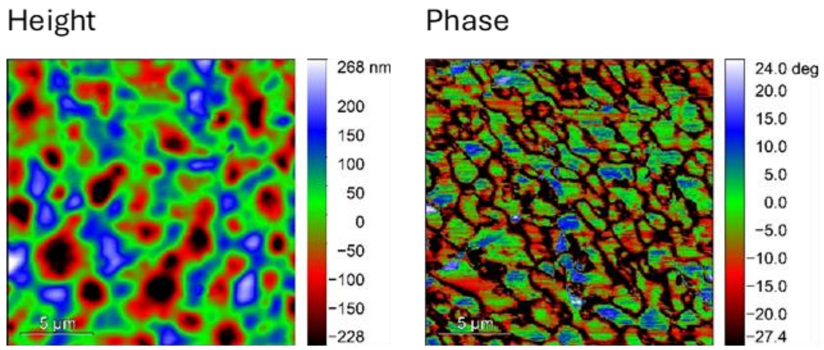

For P-NFIB 1:2

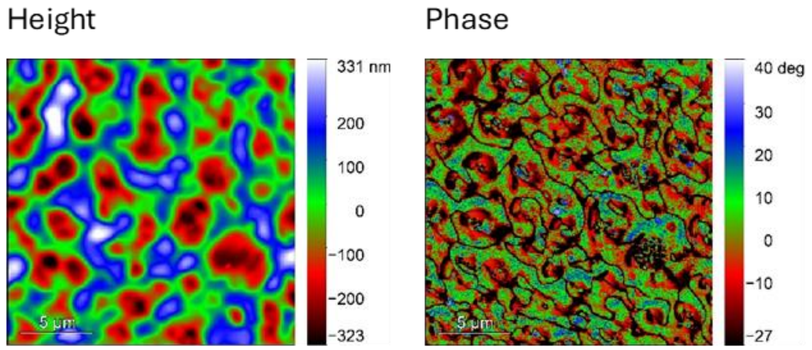

Figure S32. Colored AFM phase and height images of 1:2 and 1:4 ratios of **P–NFIB** assemblies.

Table 3. Average roughness

Polymer/DCM	Polymer/HFB	Polymer/NFIB		
Pure	Control	1:1	1:2	1:4
81 ±7	5 ±1	88 ±20	138 ±23	98 ±12

Polymer/DCM	Polymer/HFB	Polymer/PFIB		
Pure	Control	1:1	1:2	1:4
81 ±7	5 ±1	6.3 ±1	37 ±6	41 ±11

References

1. J. Skey and R. K. O'Reilly, *Chem. Commun*., 2008, **35**, 4183–4185, DOI: 10.1039/b804260h.
2. S. Perrier, *Macromolecules*, 2017, **50**, 7433–7447, DOI: 10.1021/acs.macromol.7b00767.
3. K. Ponnusamy, R. P. Babu and R. Dhamodharan, *J. Polym. Sci., Part A: Polym. Chem*., 2013, **51**, 1066–1078, DOI: 10.1002/pola.26466.
4. P. M. Lathrop, R. Sun, F. L. Beyer and Y. A. Elabd, *Macromolecules*, 2024, **57**, 3776–3797, DOI: 10.1021/acs.macromol.3c02435.
5. Y. Hou, W. Hu, X. Li, J. J. Skinner, D. Liu and K. Wüthrich, *J. Biomol*. *NMR*, 2017, **68**, 1–6, DOI: 10.1007/s10858-017-0107-8.